Precise predictions for slepton pair production

Ayres Freitas[a,b], Andreas von Manteuffel[b]

[a] *Fermi National Accelerator Laboratory, Batavia, IL 60510-500, USA*
[b] *Deutsches Elektronen–Synchrotron DESY, D–22603 Hamburg, Germany*

Abstract

At a future linear collider, the masses and couplings of scalar leptons can be measured with high accuracy, thus requiring precise theoretical predictions for the relevant processes. In this work, after a discussion of the expected experimental precision, the complete one-loop corrections to smuon and selectron pair production in the MSSM are presented and the effect of different contributions in the result is analyzed.

1 Introduction

If supersymmetric particles are detected in the future, their properties can be studied with high accuracy at a high-energy linear collider [1]. Accordingly, precise theoretical predictions for the anticipated processes are important for the determination of the couplings and the underlying supersymmetry-breaking parameters. In this report, the production of scalar leptons near threshold and in the continuum is analyzed, focusing on the production of scalar electrons (selectrons) $\tilde{e}$ and scalar muons (smuons) $\tilde{\mu}$ in e^+e^- annihilation. The possibility to produce selectrons in the e^-e^- mode is also discussed.

The status of theoretical predictions for the excitation curves near threshold, being relevant for the measurement of the slepton masses, is shortly summarized. The measurement of the cross-sections in the continuum, on the other hand, can be used to precisely determine the couplings of the sleptons. For this purpose, the complete next-to-leading order radiative corrections to the production of selectrons and smuons in the framework of the Minimal Supersymmetric Standard Model (MSSM) are presented. Numerical results are given for the $\mathcal{O}(\alpha)$ corrections to the processes $e^+e^- \to \tilde{\mu}^+_{\rm R}\tilde{\mu}^-_{\rm R}$ and $e^\pm e^- \to \tilde{e}^\pm_{\rm R}\tilde{e}^-_{\rm R}$.

2 Precision measurements near threshold

At a linear collider with high luminosity, the masses of sleptons can be determined with high accuracy by measuring the shape of the production cross-section near threshold. Previous analyses have shown that the expected experimental precision for the mass measurement is of the order $\mathcal{O}(100$ MeV) [1]. It is therefore necessary to incorporate effects beyond leading order in the theoretical predictions in order to match the experimental accuracy. Near threshold, important corrections to the cross-sections arise from the non-zero slepton width and the Coulomb corrections [2]. The slepton width $\Gamma_{\tilde{l}}$ is expected to be small compared to the slepton mass $m_{\tilde{l}}$. It can be incorporated by introducing a complex mass for the intermediate off-shell sleptons, $m^2_{\tilde{l}} \to m^2_{\tilde{l}} - im_{\tilde{l}}\Gamma_{\tilde{l}}$. The Coulomb rescattering correction is one of the most important radiative corrections near threshold arising from photon exchange between the slowly moving sleptons. For the production of off-shell sleptons with orbital angular momentum l its leading contribution is given by

Table 1: Expected precision for the determination of selectron and smuon masses and widths from measuring the threshold cross-sections at five equidistant points. The values are for the SPS1 scenario [3].

Process	Integr. Lumin. [fb^{-1}]	Mass [GeV]	Width [MeV]
$e^+e^- \to (\tilde{e}_\mathrm{R}^+\tilde{e}_\mathrm{R}^-) \to e^+e^- + \not{E}$	5×10	$m_{\tilde{e}_\mathrm{R}} = 143.0^{+0.21}_{-0.19}$	$\Gamma_{\tilde{e}_\mathrm{R}} = 150^{+300}_{-250}$
$e^-e^- \to (\tilde{e}_\mathrm{R}^-\tilde{e}_\mathrm{R}^-) \to e^-e^- + \not{E}$	5×1	$m_{\tilde{e}_\mathrm{R}} = 142.95^{+0.048}_{-0.053}$	$\Gamma_{\tilde{e}_\mathrm{R}} = 200^{+50}_{-40}$
$e^+e^- \to (\tilde{e}_\mathrm{R}^\pm\tilde{e}_\mathrm{L}^\pm) \to e^+e^-\tau\tau + \not{E}$	5×10	$m_{\tilde{e}_\mathrm{L}} = 202.2^{+0.37}_{-0.33}$	$\Gamma_{\tilde{e}_\mathrm{L}} = 240^{+40}_{-40}$
$e^-e^- \to (\tilde{e}_\mathrm{L}^-\tilde{e}_\mathrm{L}^-) \to e^-e^-4\tau + \not{E}$	5×1	$m_{\tilde{e}_\mathrm{L}} = 202.2^{+0.62}_{-0.44}$	$\Gamma_{\tilde{e}_\mathrm{L}} = 240^{+500}_{-400}$
$e^+e^- \to (\tilde{\mu}_\mathrm{R}^+\tilde{\mu}_\mathrm{R}^-) \to \mu^+\mu^- + \not{E}$	5×10	$m_{\tilde{\mu}_\mathrm{R}} = 143.0^{+0.42}_{-0.38}$	$\Gamma_{\tilde{\mu}_\mathrm{R}} = 350^{+400}_{-400}$

$$\sigma_{\mathrm{coul}} = \sigma_{\mathrm{born}}\,\frac{\alpha\pi}{2\beta_p}Q_{\tilde{f}}^2\left[1-\frac{2}{\pi}\arctan\frac{|\beta_M|^2-\beta_p^2}{2\beta_p\,\Im m\,\beta_M}\right]\Re e\left[\frac{\beta_p^2+\beta_M^2}{2\beta_p^2}\right]^l \tag{1}$$

with $\beta_p = \frac{1}{s}\sqrt{(s-p_+^2-p_-^2)^2-4p_+^2p_-^2}$, and $\beta_M = \frac{1}{s}\sqrt{(s-M_+^2-M_-^2)^2-4M_+^2M_-^2}$. Here $Q_{\tilde{f}}$, $p_\pm$ and $M_\pm^2 = m_\pm^2 - i\,m_\pm\Gamma_\pm$ are the charge, the momenta and complex pole masses of the slepton and anti-slepton.

The slepton signal is characterized by their decays into neutralinos and charginos. Here the decay channels $\tilde{l}_\mathrm{R}^- \to l^-\tilde{\chi}_1^0$ and $\tilde{l}_\mathrm{L}^- \to l^-\tilde{\chi}_2^0 \to l^-\tau\tau\tilde{\chi}_1^0$ have been considered, with the lightest neutralino $\tilde{\chi}_1^0$ escaping undetected. Important backgrounds arise both from both Standard Model and supersymmetric sources. After applying appropriate cuts to reduce the background, the slepton masses and widths can be extracted in a model-independent way from the measurement of the threshold cross-section. In Tab. 1 results are given from a fit to cross-section measurements at five equidistant center-of-mass energies near threshold. The cross-sections have been simulated including the aforementioned theoretical corrections as well as initial-state radiation in the leading-log approximation and beamstrahlung effects. The findings of this study are consistent with the numbers quoted in [4], which have been obtained without taking into account background contributions and partly with higher integrated luminosity.

3 Analysis of slepton couplings

In contrast to the masses of the superpartners, their couplings are not directly modified by soft-breaking terms. As a consequence, supersymmetry relates the Standard Model gauge coupling between a vector boson V and a fermion f, $g(Vff)$ to the gauge coupling between the vector boson V and the scalar fermion $\tilde{f}$, $\bar{g}(V\tilde{f}\tilde{f})$, as well as to the Yukawa coupling between the gaugino partner $\tilde{V}$ of the vector boson, the fermion f and the sfermion $\tilde{f}$, $\hat{g}(\tilde{V}f\tilde{f})$. Within softly broken supersymmetric theories all three kinds of (bare) couplings are required to be identical, $g = \bar{g} = \hat{g}$. The gauge and Yukawa couplings of scalar fermions can be precisely determined by measuring their production cross-sections at a linear collider. For the case of the SU(3) QCD sector in the MSSM this has been investigated in Ref. [5]. In the electroweak sector, which comprises the hypercharge $\mathrm{U}(1)_\mathrm{Y}$ coupling g_1 and the $\mathrm{SU}(2)_\mathrm{L}$ coupling g_2, the coupling relation can be accurately tested by measuring the pair-production cross-sections of scalar leptons. The pair production

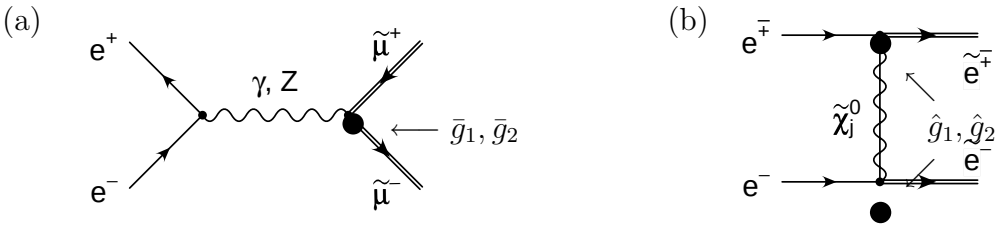

Figure 1: Slepton gauge and Yukawa couplings in tree-level contributions to smuon (a) and selectron (b) pair production. $\bar{g}_1$ and $\bar{g}_2$ denote the slepton $\mathrm{U}(1)_\mathrm{Y}$ and $\mathrm{SU}(2)_\mathrm{L}$ gauge coupling, while $\hat{g}_1$ and $\hat{g}_2$ indicate the corresponding Yukawa couplings.

for smuons, which proceeds via s-channel photon and Z-boson exchange, is particularly suited for the extraction of the slepton gauge couplings $\bar{g}_{1,2}$, see Fig. 1 (a). On the other hand, the Yukawa couplings $\hat{g}_{1,2}$ can best be probed in the production of selectrons, as a result of the t-channel neutralino exchange, see Fig. 1 (b). As mentioned above, selectron production can also be studied in e^-e^- collisions.

In order to extract the Yukawa couplings from the measurement of the selectron cross-sections, it is necessary to use information about the neutralino system. Here it is assumed that the neutralino sector has the form of the MSSM, essentially depending on the gaugino parameters M_1, M_2 and the Higgs parameter μ. The dependence on $\tan\beta = v_\mathrm{u}/v_\mathrm{d}$, the ratio of the vacuum expectation values of the two Higgs doublets, is relatively mild and can be neglected if the value of $\tan\beta$ can be extracted with moderate accuracy from some other measurement like Higgs decay branching ratios. Thus the three parameters M_1, M_2 and μ can be determined from the measurement of three chargino or neutralino masses. Here the two chargino masses and the lightest neutralino mass have been used, assuming the following—rather conservative—experimental errors: $\delta m_{\tilde{\chi}_1^\pm} = 100$ GeV, $\delta m_{\tilde{\chi}_2^\pm} = 400$ GeV, $\delta m_{\tilde{\chi}_1^0} = 100$ GeV. The total slepton cross-sections and signal-to-background ratios can be enhanced by suitable beam polarization. It is assumed that the polarization degree can be controlled up to 1%. The backgrounds are further reduced by applying appropriate cuts [2, 13]. As before, the same decay modes and final state signatures listed in the first column of Tab. 1 have been used.

The resulting constraints on the Yukawa couplings $\hat{g}_1$ and $\hat{g}_2$ from selectron cross-section measurements are depicted in Fig. 2. From the figure the following resulting accuracies are obtained:

$$e^+e^-: \quad \delta\hat{g}_1/\hat{g}_1 \approx 0.18\%, \qquad \delta\hat{g}_2/\hat{g}_2 \approx 0.8\%, \tag{2}$$

$$e^-e^-: \quad \delta\hat{g}_1/\hat{g}_1 \approx 0.23\%, \qquad \delta\hat{g}_2/\hat{g}_2 \approx 0.8\%. \tag{3}$$

On the other hand, from the measurement of the R-smuon production cross-section, the smuon gauge coupling can be extracted with a total error of 1%.

Therefore it is clearly necessary to include radiative corrections in the theoretical predictions for the slepton cross-sections in order to match the experimental accuracy. As a first step the produced sleptons may be considered on-shell, since in the continuum far above threshold the effect of the non-zero slepton width on the total cross-section is relatively small, of the order $\Gamma_{\tilde{l}}/m_{\tilde{l}}$. Thus, the production and decay of the sleptons can be treated separately. While the MSSM one-loop corrections to the decay of sleptons into

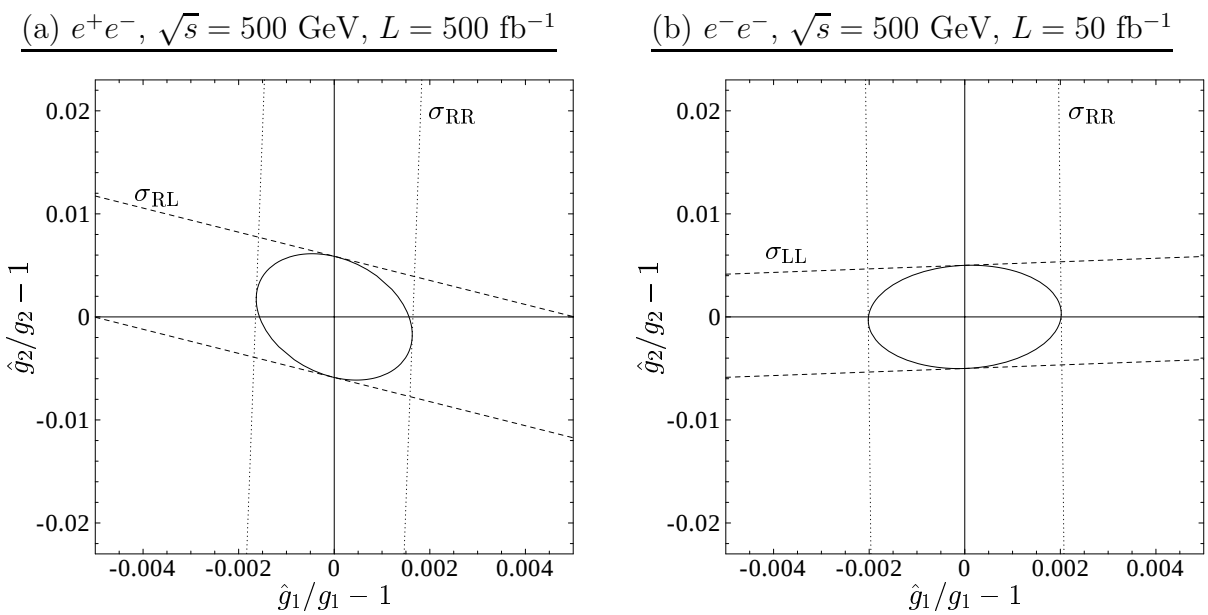

Figure 2: 1σ bounds on the determination of the supersymmetric Yukawa couplings $\hat{g}_1$ and $\hat{g}_2$ from selectron cross-section measurements. The two plots compare the information obtained from the cross-sections $\sigma_{\rm RR} = \sigma[e^+ e^- \to \tilde{e}_{\rm R}^+ \tilde{e}_{\rm R}^-]$ and $\sigma_{\rm RL} = \sigma[e^+ e^- \to \tilde{e}_{\rm R}^\pm \tilde{e}_{\rm L}^\mp]$ in the e^+e^- mode (a) as well as $\sigma_{\rm RR} = \sigma[e^- e^- \to \tilde{e}_{\rm R}^- \tilde{e}_{\rm R}^-]$ and $\sigma_{\rm LL} = \sigma[e^- e^- \to \tilde{e}_{\rm L}^- \tilde{e}_{\rm L}^-]$ in the e^-e^- mode, respectively. Values for SPS1 scenario [3].

neutralinos and charginos, $\tilde{l}^\pm \to l^\pm \tilde{\chi}_i^0$ and $\tilde{l}^\pm \to \overset{(-)}{\nu}_l \tilde{\chi}_i^\pm$, have been computed in Refs. [6, 7], the following sections will discuss the complete next-to-leading order corrections in the MSSM to the production of scalar leptons.

4 Radiative corrections and renormalization

The computation of the $\mathcal{O}(\alpha)$ corrections to scalar lepton production requires the inclusion of all sectors of the electroweak MSSM in the loop contributions. In order to reduce the number of parameters the following simplifications have been made:

All soft-breaking parameters of the MSSM are assumed to be real, i.e. only the case of CP conservation is considered. The masses of the fermions of the first two generations are neglected, and accordingly no mixing between the left- and right-chiral components of the first and second generation sfermions occurs. On the other hand, due to the large Yukawa couplings, the fermion masses and sfermion mixings in the third generation are fully taken into account. The CKM matrix is assumed to be diagonal and no flavour mixing between the sfermions is considered.

In this work the on-shell renormalization scheme has been used, which relates the mass parameters to the pole position of the propagators and the electric charge to the electron coupling in the Thompson limit. The gauge sector of the MSSM is renormalized similar to the Standard Model gauge sector. The relevant expressions can be found e.g. in Ref. [8]. For the production of scalar leptons of the first two generations, mixing between the sleptons can be neglected, as mentioned above. Accordingly, the L- and R-sleptons can be renormalized independently.

A large number of MSSM couplings and masses depend on $\tan\beta = v_\mathrm{u}/v_\mathrm{d}$. However, the vacuum expectation values and $\tan\beta$ are not physical quantities, so that it is difficult to relate $\tan\beta$ to an observable [9]. For technical reasons it is instead advantageous to renormalize $\tan\beta$ in the $\overline{\mathrm{DR}}$ scheme, which amounts to cancelling only the divergent part in dimensional reduction with the counterterm. This definition of $\tan\beta$ has been used here.

The mass spectrum of the two chargino and four neutralino states depends only on three independent parameters, the superpotential parameter μ and the gaugino parameters M_1 and M_2. In our renormalization procedure, counterterms for these parameters are introduced, which enter in the renormalization of the chargino and neutralino mass matrices. The counterterms δM_1, δM_2, $\delta\mu$ are fixed by imposing on-shell conditions for three of the six mass eigenvalues [10, 11][1], for which here the two chargino masses and the lightest neutralino mass have been chosen:

$$\begin{aligned}
\delta M_2 = \frac{1}{\mu^2 - M_2^2}\Big[&(m_{\tilde\chi_2^\pm}\mu - m_{\tilde\chi_1^\pm} M_2)\,\delta m_{\tilde\chi_1^\pm} + (m_{\tilde\chi_1^\pm}\mu - m_{\tilde\chi_2^\pm} M_2)\,\delta m_{\tilde\chi_2^\pm} \\
&+ M_2\,\delta M_\mathrm{W}^2 + \mu\,\delta\big(M_\mathrm{W}^2 \sin 2\beta\big)\Big], \\
\delta\mu = \frac{1}{M_2^2 - \mu^2}\Big[&(m_{\tilde\chi_2^\pm} M_2 - m_{\tilde\chi_1^\pm}\mu)\,\delta m_{\tilde\chi_1^\pm} + (m_{\tilde\chi_1^\pm} M_2 - m_{\tilde\chi_2^\pm}\mu)\,\delta m_{\tilde\chi_2^\pm} \\
&+ \mu\,\delta M_\mathrm{W}^2 + M_2\,\delta\big(M_\mathrm{W}^2 \sin 2\beta\big)\Big], \\
\text{with}\quad \delta m_{\tilde\chi_k^\pm} = \frac{1}{2}\,&\Re e\big\{m_{\tilde\chi_k^\pm}\Sigma_k^{\pm\mathrm{L}}(m^2_{\tilde\chi_k^\pm}) + m_{\tilde\chi_k^\pm}\Sigma_k^{\pm\mathrm{R}}(m^2_{\tilde\chi_k^\pm}) + 2\,\Sigma_k^{\pm\mathrm{S}}(m^2_{\tilde\chi_k^\pm})\big\}, \\
\delta M_1 = \frac{1}{N_{11}^2}\Big[&\Re e\big\{m_{\tilde\chi_1^0}\Sigma_1^{0\mathrm{L}}(m^2_{\tilde\chi_1^0}) + \Sigma_1^{0\mathrm{S}}(m^2_{\tilde\chi_1^0})\big\} - N_{12}^2\,\delta M_2 + 2N_{13}N_{14}\,\delta\mu \\
&+ 2N_{11}\big[N_{13}\,\delta\big(M_\mathrm{Z} s_\mathrm{W}\cos\beta\big) - N_{14}\,\delta\big(M_\mathrm{Z} s_\mathrm{W}\sin\beta\big)\big] \\
&+ 2N_{12}\big[N_{13}\,\delta\big(M_\mathrm{Z} c_\mathrm{W}\cos\beta\big) - N_{14}\,\delta\big(M_\mathrm{Z} c_\mathrm{W}\sin\beta\big)\big]\Big].
\end{aligned} \tag{4}$$

Here $\Sigma_k^{\pm\mathrm{L,R,S}}$ and $\Sigma_k^{0\mathrm{L,R,S}}$ are the left-, right-handed and scalar components of the unrenormalized self-energy of the k-th chargino and neutralino, respectively. N denotes the neutralino mixing matrix, which is taken at the tree-level since the above equations are only required at the one-loop level. For more details on the renormalization procedure, see Refs. [13, 7].

The UV-divergent loop integrals have been regularized using dimensional reduction [14], which preserves gauge invariance and supersymmetry at least up to the one-loop level. On the other hand, dimensional regularization, being widely used for Standard Model calculations, is known to violate supersymmetry, which therefore in general needs to be restored by extra counterterms. However, since dimensional regularization preserves gauge invariance, no symmetry-restoring counterterms are required for the renormalization of gauge couplings and masses. In fact, since the production of smuons only involves gauge couplings at tree-level, the one-loop corrections can directly be computed both with dimensional regularization and dimensional reduction. It has been explicitly checked that

[1] An alternative renormalization procedure has been given in Ref. [12] which is physically equivalent at the one-loop level, but differs in the definition of the renormalized parameters M_1, M_2, μ.

the results for smuon production agree for both methods. In the loop corrections to selectron production, on the other hand, there is a finite difference between the two regularization schemes. Here dimensional reduction has been used.

The computation of the loop contributions was performed using the computer algebra tools *FeynArts 3.0* [15] and *FeynCalc 2.2* [16]. Throughout the calculation, a general R_ξ gauge was used. By reducing the results to generic scalar one-loop integrals, the gauge-parameter independence was explicitly verified.

In order to obtain IR-finite and physically meaningful results, the virtual corrections to both processes have been supplemented with the real photon bremsstrahlung contributions. For the numerical analyses in the next section, the real photon emission has been treated fully inclusive.

5 Discussion of one-loop results for $\tilde{\mu}$ and $\tilde{e}$ pair production

In the following numerical results are presented in the SPS1 scenario [3]. A large part of the next-to-leading order corrections stems from universal QED contributions to the electromagnetic coupling and initial-state photon radiation. The dominant contributions to the electromagnatic coupling from light-fermion loops (i.e. all fermions except the top-quark, which decouples) can easily be incorporated by a shift $\Delta\alpha$ of the fine structure constant α. The radiation of soft and collinear photons from the incoming $e^\pm$ leads to large logarithmic corrections $\propto \log(Q/m_\mathrm{e})$ with $Q = \mathcal{O}(\sqrt{s})$. They can be taken into account by convoluting the Born cross-section with a radiator function. These universal terms are therefore dropped from the next-to-leading order result. The effect of the non-universal residual corrections is then given by

$$\Delta_\alpha = (\sigma_\mathrm{NLO} - \sigma_\mathrm{Born})/\sigma_\mathrm{Born}, \tag{5}$$

where σ_Born is the Born cross-section including the universal QED effects.

The effect of the remaining non-universal $\mathcal{O}(\alpha)$ corrections is shown in Fig. 3 for the production of R-smuons in e^+e^- annihilation and in Fig. 4 (a) and (b) for the production of R-selectrons in e^+e^- and e^-e^- collisions, respectively. The effect of the next-to-leading order contributions amounts to 5–10%.

An interesting feature of the loop corrections to selectron production is, in contrast to smuon production, the non-decoupling behaviour of supersymmetric particles in the loops. This is related to the fact that the tree-level amplitude for smuon production only involves gauge couplings, see Fig. 1 (a), whereas the t-channel diagrams to selectron production involve the electron-selectron-neutralino Yukawa coupling, cf. Fig. 1 (b). The origin of the non-decoupling effects can be illustrated by the renormalization group (RG) running of the gauge and Yukawa coupling in the $\overline{\mathrm{MS}}$ or $\overline{\mathrm{DR}}$ scheme [17]. In the following, the effect arising from quark/squark loops will be considered as an example.

Above the squark mass scale ($Q > m_{\tilde{\mathrm{q}}}$), supersymmetry is unbroken so that the gauge coupling $g(Q)$ and the Yukawa coupling $\hat{g}(Q)$ are equal. At $Q = m_{\tilde{\mathrm{q}}}$ the squarks decouple from the RG running of the couplings. While $g(Q)$ still runs for $Q < m_{\tilde{\mathrm{q}}}$ because of quark loop contributions, there is no running of $\hat{g}(Q)$ from quark/squark loops below $Q = m_{\tilde{\mathrm{q}}}$.

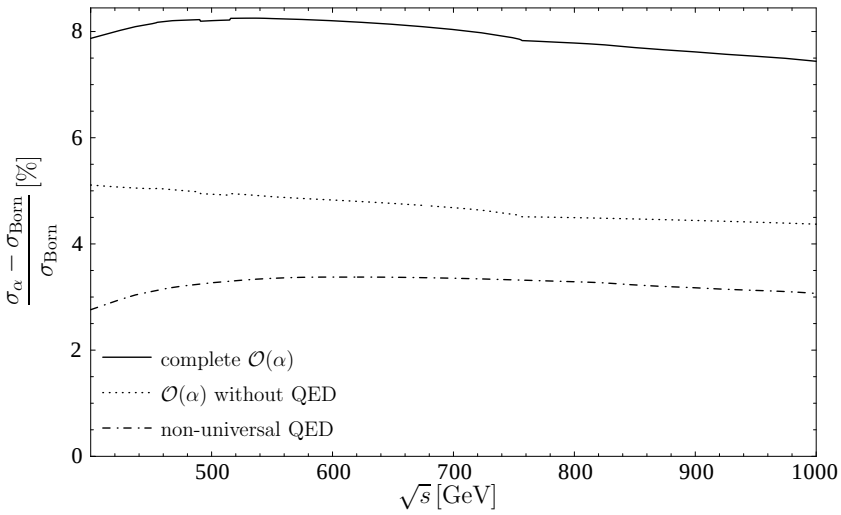

Figure 3: Electroweak corrections to the cross-section for $e^+e^- \to \tilde{\mu}_{\rm R}^+\tilde{\mu}_{\rm R}^-$, relative to the Born cross-section. Separately shown are full non-universal $\mathcal{O}(\alpha)$ contributions, the genuine weak (non-QED) corrections and the QED corrections, including soft and hard real bremsstrahlung contributions but no universal ISR terms, The input parameters are taken from SPS1 scenario [3] with $m_{\tilde{\mu}_{\rm R}} = 143$ GeV.

When comparing the two couplings at the weak scale, e.g. $Q = M_{\rm W}$, they therefore differ by a logarithmic term

$$\hat{g}(Q)/g(Q) - 1 \propto \log(m_{\tilde{\rm q}}/M_{\rm W}). \tag{6}$$

It is obvious that this contribution does not vanish in the limit of large squark masses.

As mentioned before, the computation of the loop corrections to slepton production in this work was performed in the on-shell scheme. In the on-shell scheme, all couplings are manifestly scale-invariant, so that the relation $g = \hat{g}$ remains valid to all orders of perturbation theory. Nevertheless, in this scheme, the non-decoupling logarithmic contributions are present in the loop corrections to the gauge bosons in gauge coupling vertices and to the gauginos in gaugino-lepton-slepton vertices. By comparing the effective vertices $g_{\rm eff}$ and $\hat{g}_{\rm eff}$ including one-loop corrections, one finds a corresponding relation to eq. (6),

$$\hat{g}_{\rm eff}/g_{\rm eff} - 1 \propto \log(m_{\tilde{\rm q}}/M_{\rm W}). \tag{7}$$

The effect of the squark loop contributions can also be seen in Fig. 5. As evident from the figure, the $\tilde{\mu}_{\rm R}^+\tilde{\mu}_{\rm R}^-$ cross-section does not depend on the common squark soft-breaking parameter $M_{\tilde{\rm Q}} = m_{\tilde{\rm q}_{\rm L}} = m_{\tilde{\rm u}_{\rm R}} = m_{\tilde{\rm d}_{\rm R}}$ for large values of $M_{\tilde{\rm Q}}$. On the other hand, for increasing values of $M_{\tilde{\rm Q}}$, the size of the radiative corrections to $\tilde{e}_{\rm R}^-\tilde{e}_{\rm R}^-$ production grows logarithmically. For very large values of $M_{\tilde{\rm Q}} \sim 100$ TeV, the effect of the squark loops can amount to a few percent.

In summary, the relevance of accurate theoretical predictions for the precise analysis of slepton properties at a future linear collider has been outlined. The full next-to-leading order corrections to the production of selectrons and smuons were presented and shown to be sizeable, including potentially large non-decoupling effects from superpartners in the loops.

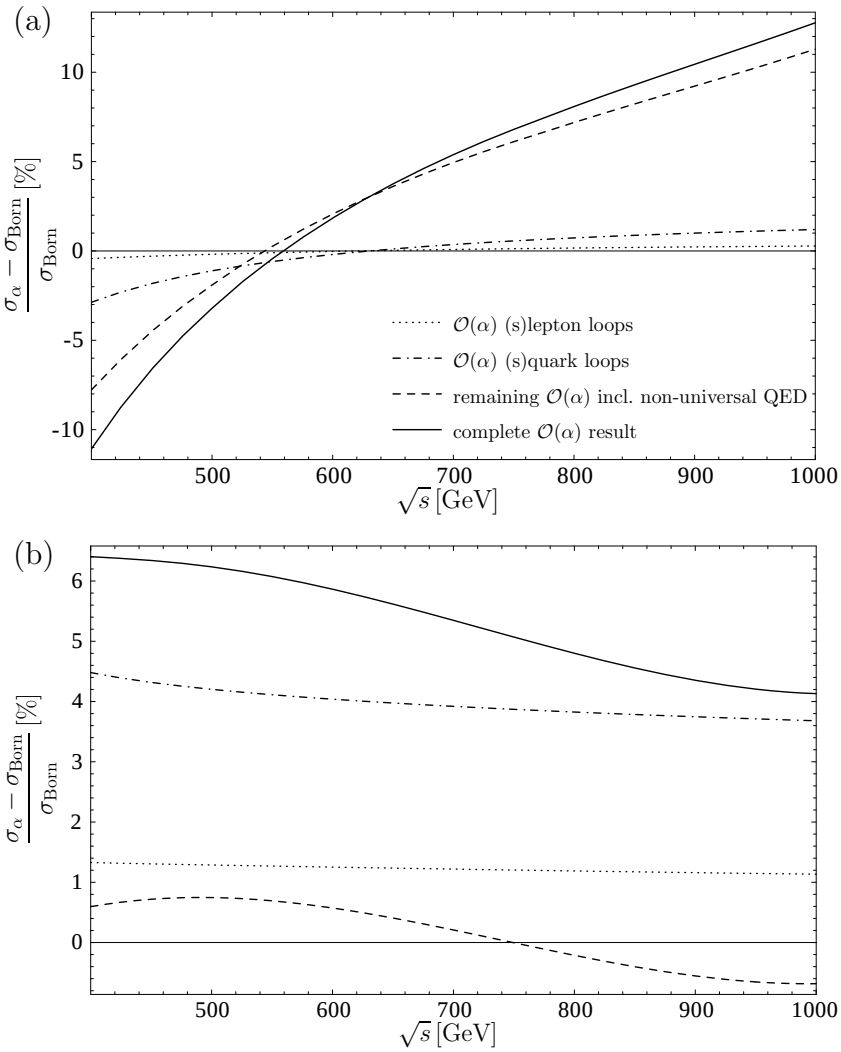

Figure 4: Electroweak corrections to the cross-section for $e^+e^- \to \tilde{e}_{\rm R}^+\tilde{e}_{\rm R}^-$ (a) and $e^-e^- \to \tilde{e}_{\rm R}^-\tilde{e}_{\rm R}^-$ (b), relative to the Born cross-sections. Besides the full non-universal $\mathcal{O}(\alpha)$ results, contributions from different subsets of diagrams are shown. The input parameters are taken from SPS1 scenario [3] with $m_{\tilde{e}_{\rm R}} = 143$ GeV.

References

[1] TESLA Technical Design Report, Part III, eds. R. Heuer, D. J. Miller, F. Richard, and P. M. Zerwas, DESY-2001-11C, [hep-ph/0106315]; T. Abe *et al.* [American Linear Collider Working Group Collaboration], in *Proc. of the APS/DPF/DPB Summer Study on the Future of Particle Physics (Snowmass 2001)* eds. R. Davidson and C. Quigg, SLAC-R-570, [hep-ex/0106056]; K. Abe *et al.* [ACFA Linear Collider Working Group Collaboration], KEK-REPORT-2001-11, [hep-ph/0109166].

[2] A. Freitas, D. J. Miller, and P. M. Zerwas, Eur. Phys. J. C **21** (2001) 361; A. Freitas and D. J. Miller, in *Proc. of the APS/DPF/DPB Summer Study on the Future of Particle Physics (Snowmass 2001)* eds. R. Davidson and C. Quigg [hep-ph/0111430].

[3] B. C. Allanach *et al.*, Eur. Phys. J. C **25** (2002) 113.

[4] H. U. Martyn and G. A. Blair, in *Proc. of the International Workshop on Linear Colliders*, Sitges, Spain (1999), [hep-ph/9910416]; H. U. Martyn, contribution to *Workshop on Physics at TeV Colliders*, Les Houches, France (1999), [hep-ph/0002290]; C. Blöchinger, H. Fraas, G. Moortgat-Pick, and W. Porod, Eur. Phys. J. C **24** (2002) 297.

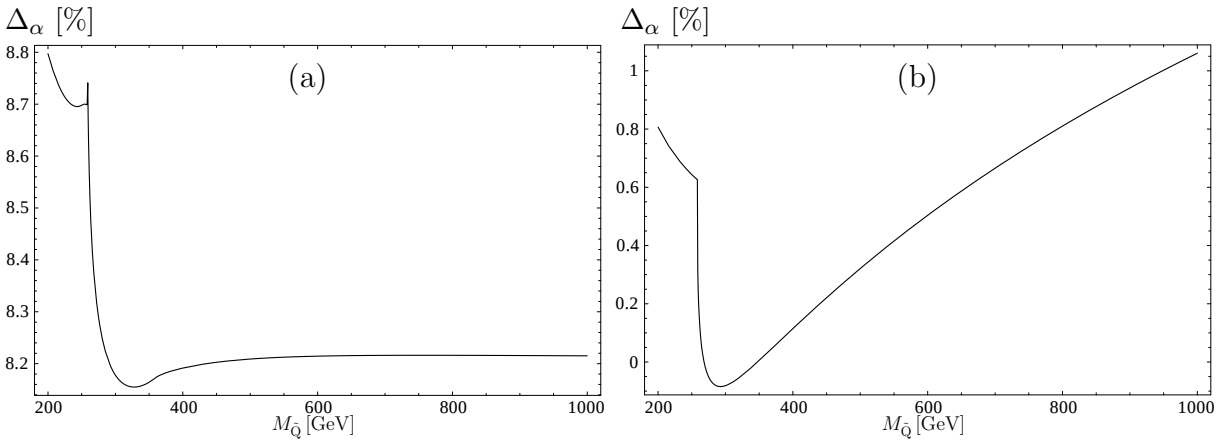

Figure 5: Dependence of the relative corrections $\Delta_\alpha = (\sigma_{\rm NLO} - \sigma_{\rm Born})/\sigma_{\rm Born}$ [in %] on the soft-breaking squark mass parameter $M_{\tilde{\rm Q}}$ for $\tilde{\mu}_{\rm R}^+\tilde{\mu}_{\rm R}^-$ production (a) and $\tilde{e}_{\rm R}^-\tilde{e}_{\rm R}^-$ production (b). The values of the other parameters are taken from the SPS1 scenario [3] and $\sqrt{s} =$ 500 GeV.

[5] A. Brandenburg, M. Maniatis, and M. M. Weber, these proceedings [hep-ph/0207278].

[6] J. Guasch, W. Hollik, and J. Solà, Phys. Lett. B **510** (2001) 211; these proceedings [hep-ph/0210120].

[7] J. Guasch, W. Hollik, and J. Solà, hep-ph/0207364.

[8] A. Denner, Fortsch. Phys. **41** (1993) 307.

[9] A. Freitas and D. Stöckinger, hep-ph/0205281, to be published in Phys. Rev. D; these proceedings [hep-ph/0210372].

[10] D. Pierce and A. Papadopoulos, Phys. Rev. D **50** (1994) 565; Nucl. Phys. B **430** (1994) 278.

[11] T. Fritzsche and W. Hollik, hep-ph/0203159.

[12] H. Eberl, M. Kincel, W. Majerotto, and Y. Yamada, Phys. Rev. D **64** (2001) 115013 [hep-ph/0104109].

[13] A. Freitas, Ph.D. thesis, Hamburg (2002), DESY-THESIS-2002-023.

[14] W. Siegel, Phys. Lett. B **84** (1979) 193; D. M. Capper, D. R. Jones, and P. van Nieuwenhuizen, Nucl. Phys. B **167** (1980) 479.

[15] T. Hahn, Comput. Phys. Commun. **140** (2001) 418; T. Hahn and C. Schappacher, Comput. Phys. Commun. **143** (2002) 54.

[16] R. Mertig, M. Böhm, and A. Denner, Comput. Phys. Commun. **64** (1991) 345.

[17] M. M. Nojiri, K. Fujii, and T. Tsukamoto, Phys. Rev. D **54** (1996) 6756; H. C. Cheng, J. L. Feng, and N. Polonsky, Phys. Rev. D **56** (1997) 6875.